Available online at www.sciencedirect.com
ScienceDirect
Journal of Volcanology and Geothermal Research 158 (2006) 281–295
Journal of volcanology and geothermal research
www.elsevier.com/locate/jvolgeores

Eruption and magma crystallization ages of Las Tres Vírgenes (Baja California) constrained by combined $^{230}Th/^{238}U$ and (U–Th)/He dating of zircon

Axel K. Schmitt [a,*], Daniel F. Stockli [b], Brian P. Hausback [c]

[a] Department of Earth and Space Sciences, UCLA, Los Angeles CA 90095-1567, USA
[b] Department of Geology, University of Kansas, Lawrence, KS 66045-7613, USA
[c] Geology Department, California State University, Sacramento CA 95819-6043, USA

Received 20 December 2005; received in revised form 23 June 2006; accepted 3 July 2006
Available online 20 September 2006

Abstract

Las Tres Vírgenes volcano is a calc-alkaline composite cone located near the main Gulf of California escarpment on the E coast of the Baja California peninsula. High-sensitivity ion microprobe U-series ($^{230}Th/^{238}U$) ages for zircon from La Vírgen tephra average 121^{+12}_{-10} ka (1σ; MSWD = 2.7), with discrete age peaks at ~100 and 160 ka. The noble gas mass spectrometric (U–Th)/He zircon age, corrected for disequilibrium and pre-eruptive storage, is 36 ± 3 ka. This result for the eruption age of La Vírgen tephra is significantly older than previously postulated historic or Holocene ages that were based on an 18th century map reference and ^{14}C dating of accidental charcoal, respectively. The new (U–Th)/He zircon age is consistent with a > 26 ± 4 ka age derived from cosmogenic He exposure dating of an overlying basaltic lava flow [Hausback, B.P. and Abrams, M.J., 1996. Plinian eruption of La Virgen Tephra, Volcán Las Tres Virgenes, Baja California Sur, Mexico. Eos, Transactions, American Geophysical Union, 77(46, Suppl.): 813–814.]. U–Pb zircon analysis of ignimbrites erupted from the adjacent Early Pleistocene La Reforma and El Aguajito calderas yielded ages of 1.38 ± 0.03 Ma (n = 12; MSWD = 1.0) and 1.17 ± 0.07 Ma (n = 23; MSWD = 1.3), respectively. No evidence for these ages is found among La Vírgen zircons, whereas pre-Quaternary zircon xenocrysts are common. The La Vírgen magma, therefore, evolved unrelated to Early Pleistocene magmatism in adjacent calderas, but assimilated local basement rocks. A gap between average Th–U and (U–Th)/He zircon ages suggests that zircon crystallization was discontinuous in the La Vírgen magma chamber. In addition, partial resorption of zircon suggests episodic thermal rejuvenation, most likely by basaltic recharge. Based on the zircon record, the > 100 ka lifetime of the thermal anomaly that sustained repeated intrusive pulses significantly exceeds the age of the last eruption. This strengthens the view that Tres Vírgenes has a potential for future eruptions.

Keywords: Gulf of California; volcanism; He-4; U-238/Th-230; zircon; magma chambers

1. Introduction

Volcán Las Tres Vírgenes is the youngest edifice of the Tres Vírgenes volcanic complex, a group of calc-alkaline composite cones located near the Gulf of California coast of the Baja California peninsula (Fig. 1). Active fumaroles and hot springs present in the area are

* Corresponding author. Tel.: +1 310 206 5760.
E-mail address: axel@argon.ess.ucla.edu (A.K. Schmitt).

0377-0273/$ - see front matter © 2006 Elsevier B.V. All rights reserved.
doi:10.1016/j.jvolgeores.2006.07.005

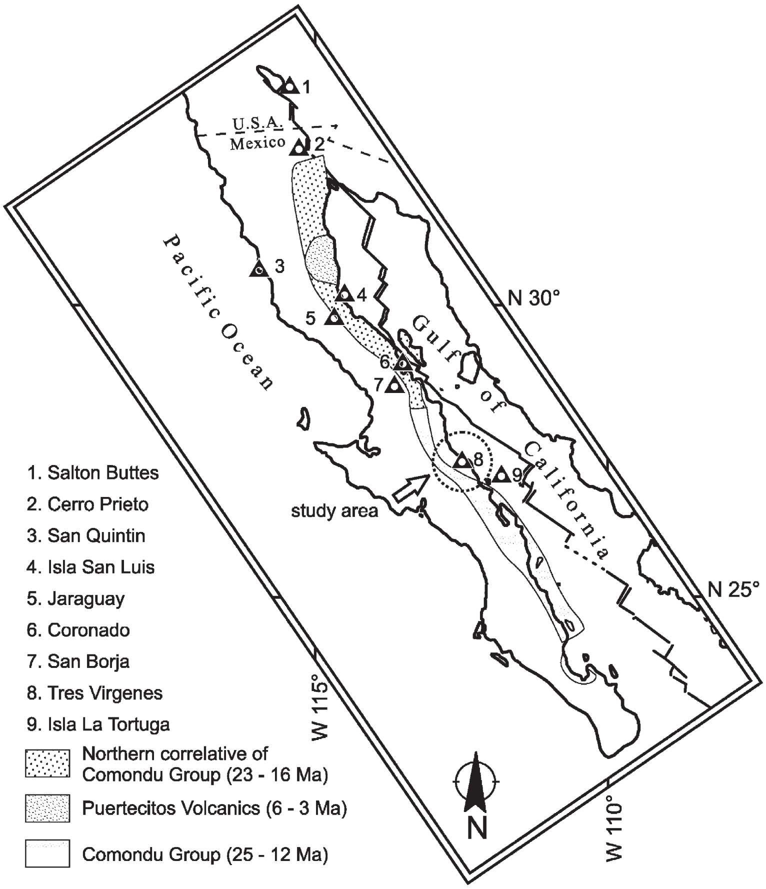

Fig. 1. Overview map of Holocene volcanic centers in Baja California and the Salton Trough showing location of Las Tres Vírgenes (modified after Medina et al., 1989; Siebert and Simkin, 2002). Fields indicate distribution of Oligocene and Miocene arc andesites and rhyolites of the Comondu group and its Northern equivalent (after Umhoefer et al., 2001), and the arc-rift transitional Puertecitos Volcanic Province (after Martín-Barajas et al., 1995). Circle indicates location of study area.

the surface manifestations of a subsurface hydrothermal system currently exploited for electric power generation (Portugal et al., 2000; Quijano-León and Gutiérrez-Negrín, 2003). Based on the 18th century map by the Jesuit missionary Ferdinando Consag (a.k.a. Ferdinand Konšćak) containing a reference to an eruption in 1746 (Ives, 1962), hydrothermal activity, and its youthful appearance, Volcán Las Tres Vírgenes is traditionally cited as one of the few historically active volcanoes along the Gulf of California rifted margin (e.g., Russell, 1897; Demant, 1984; Siebert and Simkin, 2002). Hazards from potential future eruptions of Las Tres Vírgenes include Plinian eruption columns, tephra fallout, lahars and landslides that threaten ground and air transport routes, nearby geothermal power plants, and the towns of Santa Rosalía and San Ignacio (Capra et al., 1998).

Radiometric age estimates for Las Tres Vírgenes eruptions range between ~6.5 ka (^{14}C age of charcoal; Capra et al., 1998) and ~26 ka (cosmogenic He exposure age of a basaltic lava flow; Hausback and Abrams, 1996). These ages appear inconsistent with an inferred historic eruption (Ives, 1962), although the historic eruption account is not specific and may refer to the eruption of the latest andesite summit lavas of Las Tres Vírgenes. The nature of the subsurface magmatic system that represents the heat source for the geothermal system remains equally elusive, leaving the question unanswered whether Las Tres Vírgenes is fed by a large, long-lived magma body or small, transient magma batches.

In order to better constrain crystallization and eruption ages, we explored and combined ^{230}Th/^{238}U and (U–Th)/He dating of zircon of La Vírgen tephra, the most voluminous pyroclastic deposit that erupted from Las Tres Vírgenes (Hausback and Abrams, 1996). This approach is based on the vastly different diffusive properties of radiogenic parents and daughters in zircon: Th, U (and Pb) are virtually unaffected by crystal residence at magmatic temperatures (~800 °C), whereas fast-diffusing He only accumulates after cooling to ambient temperatures following the eruption. The use of nearly non-destructive ion microprobe $^{230}Th/^{238}U$ analysis (only ~0.1% of the mass of a typical zircon is consumed during the measurement) allows us to use the same crystals for subsequent noble gas mass spectrometric analysis. Our results for La Vírgen tephra are inconsistent with a previously inferred Holocene (Capra et al., 1998) eruption age and instead demonstrate that the last violent eruption of Volcán La Vírgen occurred at ~36±3 ka (1σ error) due to thermal rejuvenation of ~100–160 ka old differentiated intrusions.

2. Geologic background

Volcán Las Tres Vírgenes is part of a volcanic cluster that includes the central vent edifices of El Azufre and El Viejo (collectively known as Tres Vírgenes Volcanic Complex; Capra et al., 1998), and the adjacent caldera structures of Aguajito and La Reforma (Demant, 1981; Demant, 1984; Garduño-Monroy et al., 1993). Off-shore volcanic ridges extending from Tres Vírgenes–Aguajito–La Reforma towards sea-floor spreading centers in the Guayamas basin (Fabriol et al., 1999) are potentially part of the same "leaky transform" system (Batiza, 1979). On-shore, the basement comprises Cretaceous granodiorite (dated by K–Ar to 91.2± 2.1 Ma; Schmidt, 1975) which is overlain by the volcano-sedimentary successions of the Miocene Comondú group and the Upper Miocene Santa Lucía andesites (Garduño-Monroy et al., 1993). During the Late Miocene, alkaline–tholeiitic compositions superseded earlier calc-alkaline volcanism following the cessation of Pacific Plate subduction and initiation of Proto-Gulf of California rifting at around ~12 Ma (Fig. 1; Hausback, 1984; Saunders et al., 1987; Sawlan, 1991). Magmas erupted from the Las Tres Vírgenes–Aguajito–La Reforma centers, however, are anomalous because they are calc-alkaline in the absence of ongoing subduction. Tres Virgenes–Aguajito–La Reforma is the largest and most recent of several isolated volcanic centers that retained a calc-alkaline geochemical signature after subduction ceased. Remelting of subduction modified mantle sources during rifting has been

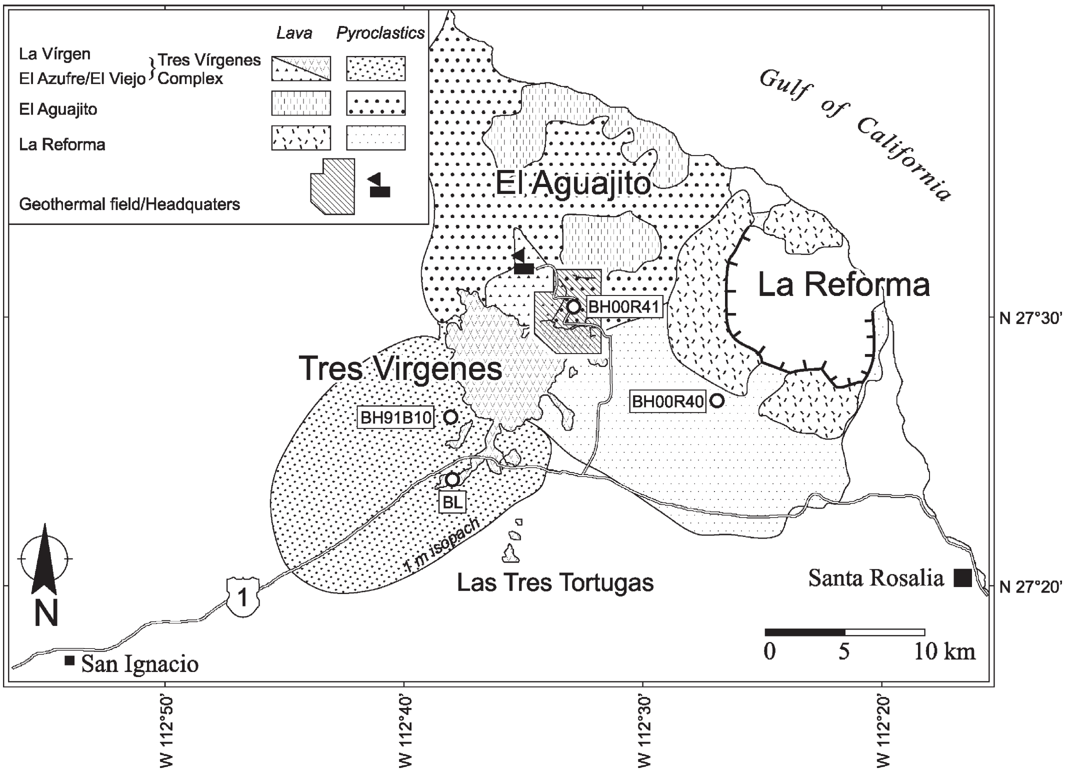

Fig. 2. Geologic map of the Tres Vírgenes Volcanic Complex (TVCC) and adjacent Aguajito and La Reforma calderas (modified after Garduño-Monroy et al., 1993; Capra et al., 1998). 1-m-isopach line drawn for La Vírgen tephra deposit. Sample localities and the location of the geothermal area are indicated: "BL" refers to the Highway Basalt locality, previously dated by cosmogenic He exposure methods (Hausback and Abrams, 1996), all others are samples from this study.

proposed as an explanation for the presence of calc-alkaline geochemical signatures in the absence of ongoing subduction (Sawlan, 1991).

Voluminous silicic volcanic activity in the area is thought to have commenced in the Early Pleistocene (1.6–1.4 Ma for intrusive and extrusive rocks at La Reforma; Schmidt, 1975; Garduño-Monroy et al., 1993). This is consistent with the reversed magnetic polarity reported for La Reforma ignimbrite (Sawlan, 1986). Progressively younger eruptions were fed by counter-clockwise migrating eruptive vents from SE to NW and NW to SW. Volcanics from Aguajito yielded K–Ar ages between 0.5 and 0.7 Ma (Garduño-Monroy et al., 1993), whereas El Viejo, El Azufre and Las Tres Vírgenes lavas range from 0.44 Ma to recent (Portugal et al., 2000). An andesitic lava flow from the NW flank of Las Tres Vírgenes also falls into the normal polarity Brunhes epoch (<780 ka; Sawlan, 1986).

Accounts on the geology of La Reforma can be found in Schmidt (1975) and Demant (1981), and a recent remote sensing mapping by Hook et al. (2005), whereas the geology of Aguajito complex has been described by Garduño-Monroy et al. (1993). In brief, voluminous silicic ignimbrites erupted from La Reforma and Aguajito that caused the formation of caldera structures. Both centers also include lava flows and cinder cones of less evolved composition, as well as dacitic–rhyolitic domes inferred to outline caldera ring-fault structures (Garduño-Monroy et al., 1993).

The formation of the ~15 km^3 Las Tres Vírgenes volcano (Sawlan, 1986; Capra et al., 1998) initiated with an early volcano-building stage of andesitic–dacitic effusive activity, followed by pyroclastic eruptions of dacitic–rhyolitic pumice and juvenile clasts of the La Vírgen tephra (Hausback and Abrams, 1996). The eruptive sequence terminated with the localized emplacement of south flowing basalt and basaltic–andesitic lava flows (Sawlan, 1986; Hausback and Abrams, 1996).

3. Methods

Pumice clasts from the La Vírgen fall deposit were sampled from the lower portion of a ~5-m-thick outcrop (sample BH91B10; Fig. 2). In addition, two whole-rock ignimbrite samples from Aguajito and La Reforma (samples BH00R40 and BH00R41; Fig. 2) were included in this study. Pumice and rock fragments were hand-picked to avoid lithic clasts and other extraneous materials, ultrasonically cleaned, dried and crushed. Zircon grains typically between ~100 and ~200 μm long were separated from the <250 μm sieved fraction using heavy liquids, magnetic separation and hand-picking.

U–Th disequilibrium dating was performed on individual zircons using the UCLA Cameca ims 1270 secondary ion mass spectrometer (SIMS, ion microprobe), modifying a technique from Reid et al. (1997). A ~40–50 nA mass-filtered O^- beam was focused into a ~35×30 μm oval spot. Secondary ions were accelerated at 10 keV with an energy bandpass of 50 eV and analyzed at a mass resolution of ~4800 using an axial electron multiplier collector in peak jumping mode. For each session, relative sensitivities for ^{238}UO and ^{232}ThO were calibrated by measuring the radiogenic ^{206}Pb/^{208}Pb ratio of concordant reference zircons AS-3 and 91500 (Paces and Miller, 1993; Wiedenbeck et al., 1995). Raw intensities were corrected for electron multiplied dead-time (25 ns). Background corrections for ^{230}ThO were performed using the averaged intensities measured on two mass stations at 244.038 and 246.300 amu (see Appendix). Elevated backgrounds at 244.038 (^{232}ThC$^+$) occur in the case of partial beam overlap with epoxy and correlate with unusually high intensities at mass 246.028 (^{230}ThO$^+$) that result from a quasi-isobaric interference ($^{232}Th_2CO^{2+}$; see Appendix). In one case, the analysis had to be discarded because of an unusually high 244.038 intensity (~5 cps) resulting from partial overlap with epoxy. Intermittently analyzed Proterozoic zircons AS-3 and 91500 yielded (^{230}Th)/(^{238}U) activities (noted by parentheses) that were in equilibrium within uncertainty (see Appendix).

La Vírgen zircons found to be in secular equilibrium and zircons from the older Aguajito and La Reforma complexes were analyzed for U–Pb using techniques outlined in Schmitt et al. (2003). U concentrations were calculated from $UO^+/^{94}Zr_2O^+$ (U–Pb analysis protocol) and $UO^+/^{90}Zr_2O_4^+$ (U–Th analysis protocol) ratios, respectively. The relative sensitivity for U and Zr was determined on 91 500 reference zircon (81.2 ppm U; Wiedenbeck et al., 1995). In addition, whole-rock U and Th concentrations and ^{230}Th/^{232}Th for La Vírgen tephra were determined by thermal ionization mass spectrometry (TIMS) and SIMS methods (Layne and Sims, 2000), respectively.

He, U and Th abundances in single zircons and zircon aliquots from La Vírgen tephra were measured using isotope dilution at the University of Kansas noble gas mass spectrometry lab. Farley et al. (2002) demonstrated the potential of the (U–Th)/He dating method as a powerful tool for dating young volcanic deposits. However, they also pointed out that (U–Th)/He ages computed assuming secular equilibrium in young zircons may lead to a systematic underestimation of the eruption age of young (<1 Ma) volcanic deposits. This age inaccuracy can be attributed to initial ^{230}Th

Table 1
U–Th results for La Vírgen tephra zircons and composite pumice sample (whole-rock). Ages calculated from two-point isochrons through zircon and whole-rock compositions

Sample BH91B10 (La Vírgen)	Grain	Spot	$^{230}Th/^{232}Th$	±	$^{238}U/^{232}Th$	±	Age (ka)	+ (ka)	− (ka)	U (ppm)	Th (ppm)
zircon	1	1	4.29	1.13	8.24	0.07	65	37	−27	56	21
zircon	1	2 [a]	3.45	0.74	6.13	0.08	69	36	−27	178	88
zircon	3	1	3.37	0.31	4.25	0.05	141	49	−34	252	180
zircon	6	1	3.12	0.44	4.68	0.03	91	37	−27	178	115
zircon	6	2	6.24	1.12	7.36	0.05	189	∞	−76	84	35
zircon	6	3 [a]	4.38	0.50	6.24	0.08	112	34	−26	227	111
zircon	6	4 [a]	3.86	0.27	4.65	0.06	166	48	−33	393	257
zircon	6	5 [a]	5.02	0.53	5.56	0.07	233	∞	−77	273	149
zircon	7	1	2.63	0.24	3.10	0.01	160	80	−46	227	223
zircon	8	1	4.89	0.25	4.47	0.04	∞	∞	∞	494	336
zircon	10	1	5.83	0.54	6.21	0.09	289	∞	−100	183	90
zircon	10	2	2.98	0.11	3.57	0.03	160	25	−20	683	582
zircon	10	3	4.27	0.23	4.79	0.06	215	69	−42	332	210
zircon	11	1	5.05	0.24	7.71	0.10	100	11	−10	646	254
zircon	12	1	3.30	0.25	4.57	0.11	110	25	−20	335	223
zircon	12	2	2.60	0.14	3.65	0.03	98	16	−14	473	394
zircon	13	1	3.80	0.26	5.91	0.08	91	14	−13	433	222
zircon	14	1	2.00	0.11	2.92	0.02	77	14	−13	600	625
zircon	15	1	9.53	2.23	8.81	0.08	∞	∞	∞	157	54
zircon	17	1	5.20	0.81	7.11	0.06	126	61	−39	56	24
zircon	18	1	2.98	0.13	3.68	0.05	144	25	−20	757	625
zircon	19	1	4.07	0.27	4.03	0.05	∞	∞	∞	237	179
whole-rock	–	–	1.085	0.022	1.095	0.011	–	–	–	1.33	3.68

Activity and age calculations used the following decay constants: λ_{230}: $9.1577 \cdot 10^{-6}$ a^{-1}; λ_{232}: $4.9475 \cdot 10^{-11}$ a^{-1}; λ_{238}: $1.55125 \cdot 10^{-10}$ a^{-1};∞ indicates secular equilibrium.

Zircon analyses by ion microprobe; whole-rock (^{230}Th)/(^{232}Th) by ion microprobe, (^{238}U)/(^{232}Th) by isotope dilution thermal ionization mass spectrometry.

[a] reanalyzed after regrinding of ~5 μm and repolishing.

deficit in zircon, resulting in slower He production than expected at secular equilibrium. ^{226}Ra may also be fractionated from its parent, ^{230}Th, but the effects of ^{226}Ra disequilibrium on zircon (U–Th)/He ages from La Vírgen tephra should be negligible in light of the age of the eruption (>10 ka) (Farley et al., 2002).

Using the measured whole-rock and zircon (^{232}Th)/(^{238}U) ratios for the La Vírgen tephra, we estimated the initial (^{230}Th)/(^{238}U) activity ratio of magmatic zircons at the time of the eruption (eruption D_{230} of Farley et al., 2002). In using this approach, we assumed that (1) the measured whole-rock value is representative of the magma from which the zircons crystallized, (2) the magma was in secular equilibrium, and (3) that we can iteratively calculate an accurate magma residence time from the independently constrained disequilibrium age of ~120 ka.

The fact that these analyses include zircons that have been removed from their epoxy mounts after SIMS measurements introduces a minor complication for the α-ejection correction to (U–Th)/He ages, which is based on the dimensions of unmodified crystals (Farley et al., 1996). We used a modified α-ejection correction procedure applying a Monte-Carlo method accounting for internal and external surfaces of the polished zircon grains (Table 1). For unpolished grains we employed a standard α-ejection correction for unmodified zircon crystals assuming a homogenous U and Th distribution (Farley et al., 1996).

4. Results

The whole-rock composition of La Vírgen tephra plots on the equiline within analytical uncertainty (Fig. 3). In contrast, most of the analyzed La Vírgen zircons are not in secular equilibrium (Table 2) and fall below the equiline in Fig. 3. Four unknowns that yielded equilibrium values within 1σ measurement uncertainty were subsequently analyzed for U–Pb. Three of these zircons yielded Pre-Quaternary U–Pb ages that range from ~25 to 250 Ma. For the remaining unknown (g10 spot s1) with a U–Th age of $289^{+\infty}_{-100}$ ka, a Late Pleistocene U–Pb age of 127±81 ka was determined. This age is consistent with the U–Th result

Table 2
Equilibrium and corrected (U–Th)/He results for La Vírgen tephra zircons

Sample name	p/b	U (ppm)	Th (ppm)	Th/U	D_{230}	D_{230} eruption	Total He (mol/g)	FT	Mass (μg)	Eq. age (ka)	± (ka)	Age (ka)	± (ka)
BH91B10p-Zr6	p	35	19	0.53	0.19	0.61	5.29×10^{-12}	0.79	13.5	31.4	1.9	40.1	2.4
BH91B10b-Zr1	b	107	59	0.55	0.19	0.61	1.70×10^{-11}	0.82	13.9	31.7	1.9	40.3	2.4
BH91B10b-Zr2	b	128	118	0.92	0.32	0.70	1.73×10^{-11}	0.80	23.2	25.6	1.6	30.4	1.9
BH91B10b-Zr3	b	73	38	0.52	0.18	0.60	1.22×10^{-11}	0.85	59.7	32.4	2.0	41.6	2.5
BH91B10p-Zr7,11	p	53	38	0.72	0.25	0.65	7.12×10^{-12}	0.71	9.4	30.1	1.8	37.3	2.3
BH91B10p-Zr12	p	106	81	0.77	0.27	0.66	1.46×10^{-11}	0.76	10.1	28.4	1.7	34.7	2.1
BH91B10p-Zr14	p	105	93	0.88	0.31	0.68	1.71×10^{-11}	0.84	33.3	29.6	1.8	35.5	2.2
BH91B10p-Zr8, 13	p	51	33	0.66	0.23	0.66	6.86×10^{-12}	0.84	52.0	25.7	1.6	31.7	1.9

Note: Column p/b denotes if samples were polished zircons plucked from ion probe mount (p) or unpolished bulk zircon crystals (b). D_{230} is the initial (^{230}Th/^{238}U]) activity ratio as estimated from the ratio of (^{232}Th/^{238}U)$_{zircon}$/(^{232}Th/^{238}U)$_{magma}$, whereas D_{230} eruption is the ratio back-calculated to the time of eruption, taking into account a magma residence time (using approach by Farley et al., 2002). FT is the standard (for *b* samples) or modified (for p samples) α-ejection correction (Farley et al., 1996). Eq. age (±1σ) stands for equilibrium (U–Th)/He calculated for initial secular equilibrium. Age (±1σ) represents the disequilibrium-corrected zircon (U–Th)/He eruption age of the Las Vírgen tephra, assuming a zircon crystallization age of 120±20 ka.

despite the large uncertainty resulting from low radiogenic Pb yield. U concentrations in zircon range between ~60 and 750 ppm with an average of ~300 ppm (Table 2) and are roughly similar to those reported for zircon in calc-alkaline rhyodacitic rocks (e.g., Mount Mazama; Bacon and Lowenstern, 2005).

Disequilibrium ages for La Vírgen zircon were calculated in two ways: by regression through all data points (excluding pre-Quaternary grains; Fig. 3) and by determining the slope of two-point isochrons through the whole-rock and zircon values. On average, both methods yield ages in close agreement (121^{+12}_{-10} and 118^{+15}_{-13} ka, respectively) with MSWD values (~2.5 in both cases) significantly beyond the 95% likelihood interval (Mahon, 1996), indicating additional, non-analytical scatter in the population. The bimodal distribution in the age histogram and probability density plots (Fig. 4) suggests the presence of two main Late Pleistocene zircon populations. Using the mixing algorithm of Sambridge and Compston (1994), ages of 96^{+7}_{-6} and 161^{+14}_{-13} ka are obtained that correspond closely to the two peaks in the probability density curve (Fig. 4). Multiple analyses on grain 10 (Fig. 5) yielded ages that range from 160^{+25}_{-20} ka (rim) to $289^{+\infty}_{-100}$ ka (core). Although these ages overlap within 2σ uncertainty,

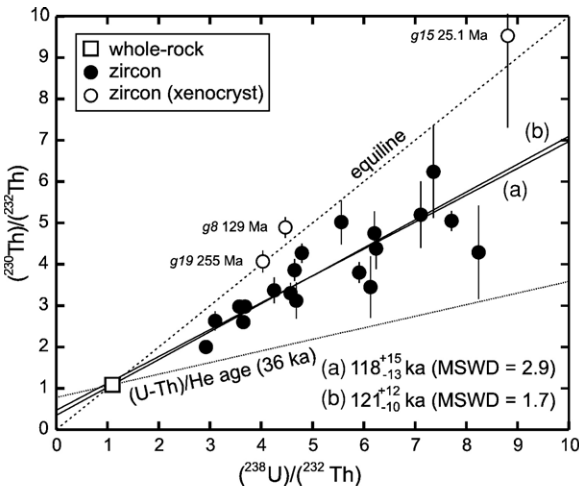

Fig. 3. (^{230}Th)/(^{232}Th) vs. (^{230}Th)/(^{238}U) isochron diagram for La Vírgen tephra zircons and composite whole-rock pumice. Free-fit (a) and average whole-rock — zircon model (b) isochrons with corresponding ages indicated. Pre-Quaternary xenocrysts (open symbols) in secular equilibrium are labeled with their respective ^{206}Pb/^{238}U ages. Error bars 1σ.

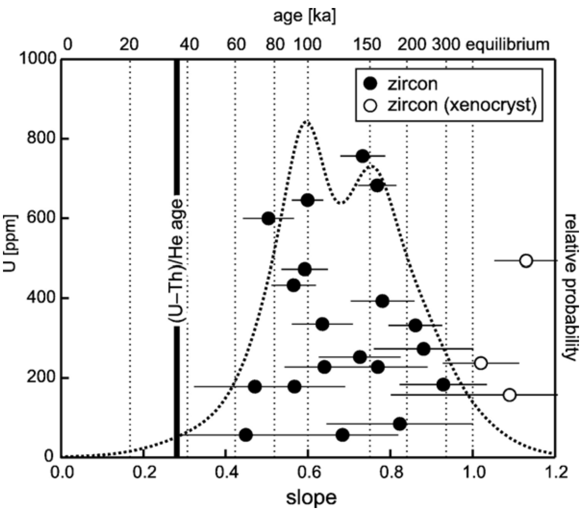

Fig. 4. Zircon U-concentration vs. two-point isochron slope and corresponding ages for La Vírgen tephra zircons. Eruption age from (U–Th)/He dating of zircon is indicated by vertical bar and probability density curve for U–Th zircon ages is plotted as thick dotted line.

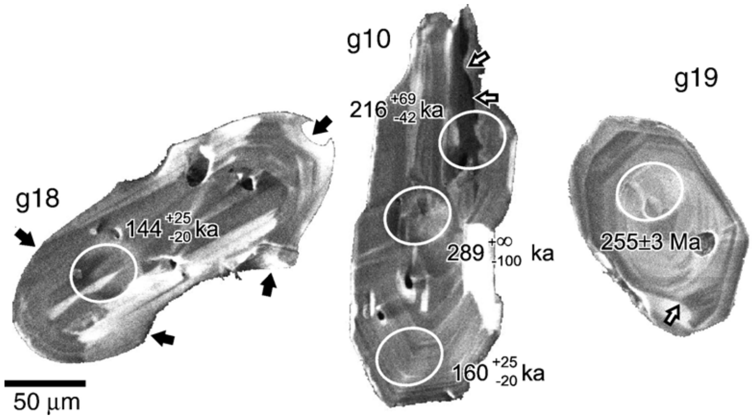

Fig. 5. Cathodoluminescence images of La Vírgen zircons. Note within grain resorption boundaries (white arrows) and rounded outer margins with truncations of growth zonation (dark arrows). Location of ion microprobe spots and U–Th model ages are indicated by white ovals.

resorption and overgrowth textures visible in the CL image of grain 10 (Fig. 5) suggest that individual crystals may record growth periods that could be separated by several 10,000 years.

Due to their relatively low U contents (average ~250 ppm; Table 3), zircons from Aguajito and La Reforma ignimbrites yielded radiogenic ^{206}Pb typically <80% (Fig. 6; Table 3). Regression ages after correction for initial disequilibrium (Schmitt et al., 2003) are 1.38 ±0.03 Ma (n=12; MSWD=1.0) and 1.17± 0.07 Ma (n=23; MSWD=1.3), suggesting homogeneous zircon populations in each sample within analytical uncertainty. Notably, pre-Quaternary zircons are absent in the Aguajito and La Reforma samples, and zircons with U–Pb ages equivalent to those found in Aguajito and La Reforma are lacking in the La Vírgen sample.

Eight single-grain laser zircon (U–Th)/He analyses from polished and unmodified bulk samples from La Vírgen yielded an average equilibrium (U-Th)/He age of 29±2 ka (MSWD=2.4). This date, however, represents a minimum age because initial disequilibrium (^{230}Th deficit due to fractionation between Th and U during zircon crystallization) is not accounted for (Farley et al., 2002). Using SIMS zircon and TIMS whole-rock U/Th values, mineral–magma partitioning coefficients are calculated that allow an estimate of the initial (^{230}Th) to be ~20% of the equilibrium value. On the other hand, pre-eruptive zircon residence will mitigate the initial disequilibrium of ^{230}Th (Farley et al., 2002). From the difference between the Th–U zircon crystallization (using an average age of 120±20 ka; see above) and the (U–Th)/He eruption ages, we estimate that at the time of the eruption (^{230}Th) had increased to ~65±5% of the equilibrium value. The weighted mean of all ^{230}Th-deficit corrected zircon (U–Th)/He ages yields an eruption age for the La Vírgen tephra of 36±3 ka (Table 1 and Fig. 7).

5. Discussion

5.1. Eruption age of La Vírgen tephra

Previous age determinations on minerals or glasses from La Vírgen pumice were hampered by the lack of suitable high-K phases such as sanidine for K–Ar or ^{40}Ar/^{39}Ar dating. There are, however, published results based on indirect dating methods: ^{14}C dating of a single carbonized wood fragment found within the middle section of the La Vírgen deposit (Capra et al., 1998) and cosmogenic He dating of basalt lava locally covering the La Vírgen deposit (location BL in Fig. 2), therefore providing a minimum age estimate for the eruption age of the La Vírgen tephra (Hausback and Abrams, 1996). The ages obtained by these methods (6515±75 yr B.P. and >26±4 ka, respectively) are inconsistent with each other and Consag's map interpreted as evidence for an historic eruption (Ives, 1962). Our disequilibrium-corrected (U–Th)/He age of 36±3 ka, however, is in agreement with the cosmogenic He surface exposure age. In fact, a potential systematic bias of He surface exposure ages to younger ages from unaccounted denudation suggests that the time gap between the La Vírgen eruption and emplacement of the basalt flow could have been rather short, on the order of several 1000 years or less.

There are precedents for problematic ^{14}C charcoal dates that dramatically underestimated the age of a deposit because of sample alteration and physical translocation (Bird et al., 2002). The relation of the Capra et al. (1998) carbonized wood fragment to the La

Table 3
U–Pb results for La Reforma, Aguajjto and La Vírgen zircons

Unit	Sample	Grain	Spot	$^{206}Pb/^{238}U$ ($\times 10^{-3}$)	± ($\times 10^{-3}$)	$^{207}Pb/^{235}U$ ($\times 10^{-3}$)	± ($\times 10^{-3}$)	cc	$^{207}Pb/^{206}Pb$	±	$^{204}Pb/^{206}Pb$ ($\times 10^{-3}$)	± ($\times 10^{-3}$)	% radiogenic ^{206}Pb	*f*	Age (Ma)	± (Ma)	U (ppm)	Th (ppm)
La Reforma	BH00R40	1	1	0.917	0.166	72.0	15.8	0.68	0.569	0.093	37.6	15.4	33.1	1.05	2.05	1.39	93	34
	BH00R40	3	1	0.333	0.027	17.4	2.8	0.86	0.379	0.037	73.9	16.2	57.5	1.06	1.31	0.23	805	768
	BH00R40	5	1	0.418	0.055	25.1	6.1	0.86	0.435	0.063	39.3	14.9	50.2	1.07	1.44	0.49	216	104
	BH00R40	7	1	0.249	0.015	6.4	1.1	0.80	0.188	0.025	43.3	9.2	81.9	1.06	1.39	0.11	1272	1111
	BH00R40	7	2	0.199	0.006	2.53	0.26	0.57	0.092	0.008	32.6	5.3	94.1	1.05	1.26	0.04	1181	1574
	BH00R40	8	1	0.534	0.068	38.0	7.9	0.74	0.517	0.074	32.9	14.8	39.8	1.07	1.46	0.63	158	63
	BH00R40	9	1	0.272	0.015	9.30	1.16	0.55	0.248	0.026	21.2	8.2	74.2	1.07	1.39	0.12	212	106
	BH00R40	9	2	0.286	0.016	10.1	2.2	0.76	0.256	0.045	23.0	10.3	73.2	1.07	1.44	0.16	443	253
	BH00R40	19	1	0.499	0.065	30.8	5.4	0.87	0.447	0.039	110	31	48.8	1.06	1.66	0.51	136	57
	BH00R40	19	2	0.466	0.060	27.0	4.8	0.85	0.419	0.041	24.1	12.0	52.3	1.06	1.66	0.47	136	64
	BH00R40	20	1	0.756	0.145	59.5	13.3	0.89	0.571	0.059	59.8	23.4	33.0	1.06	1.70	1.19	99	36
	BH00R40	21	1	0.901	0.183	93.9	20.2	0.87	0.756	0.081	79.7	25.1	9.2	1.18	0.63	1.63	129	48
Aguajito	BH00R41	1	1	1.48	0.29	149	29	0.89	0.734	0.067	57.7	18.5	12.0	1.09	1.24	2.46	68	19
	BH00R41	2	1	0.943	0.149	66.1	14.0	0.86	0.508	0.056	34.0	11.6	41.0	1.04	2.59	1.24	167	48
	BH00R41	2	2	0.431	0.028	33.4	1.8	0.29	0.562	0.040	63.2	14.0	34.1	1.10	1.04	0.21	159	55
	BH00R41	3	1	0.940	0.167	90.8	21.0	0.91	0.700	0.071	29.9	10.9	16.4	1.10	1.09	1.59	131	43
	BH00R41	4	1	0.612	0.119	55.1	11.3	0.86	0.652	0.069	43.8	14.7	22.5	1.11	0.98	1.00	215	87
	BH00R41	5	1	0.971	0.199	95.9	22.5	0.92	0.717	0.068	56.3	14.2	14.3	1.11	0.99	1.80	167	57
	BH00R41	6	1	0.479	0.081	41.7	9.2	0.85	0.632	0.075	31.1	19.8	25.1	1.12	0.87	0.73	183	61

	BH00R41	7	1	0.612	0.105	53.2	12.1	0.90	0.630	0.066	54.7	20.9	25.4	1.10	1.10	0.96	148	50
	BH00R41	9	1	0.452	0.060	33.4	6.7	0.83	0.536	0.063	30.3	12.8	37.3	1.09	1.19	0.54	170	49
	BH00R41	9	2	0.270	0.015	14.8	2.9	0.42	0.399	0.072	44.9	17.1	54.9	1.09	1.04	0.19	140	72
	BH00R41	11	1	0.554	0.106	50.1	12.3	0.91	0.656	0.069	77.7	24.0	22.1	1.12	0.88	0.97	194	85
	BH00R41	12	1	0.376	0.044	29.2	7.1	0.82	0.563	0.091	46.8	16.3	33.9	1.11	0.91	0.49	233	117
	BH00R41	13	1	0.902	0.060	89.9	9.8	0.84	0.724	0.047	58.9	12.2	13.4	1.09	0.85	0.67	259	246
	BH00R41	14	1	0.458	0.050	40.3	6.0	0.78	0.638	0.060	48.0	14.2	24.3	1.12	0.81	0.47	258	148
	BH00R41	15	1	0.417	0.032	32.5	3.5	0.84	0.565	0.034	46.9	10.9	33.6	1.10	0.99	0.28	219	125
	BH00R41	16	1	0.748	0.142	76.4	17.8	0.91	0.740	0.074	42.4	14.2	11.3	1.18	0.64	1.35	161	54
	BH00R41	17	1	0.676	0.107	62.9	12.0	0.84	0.674	0.070	30.1	12.7	19.7	1.11	0.95	0.96	190	84
	BH00R41	18	1	0.591	0.093	56.0	11.6	0.88	0.687	0.070	37.8	12.4	18.1	1.13	0.78	0.89	240	114
	BH00R41	19	1	0.956	0.165	90.3	18.0	0.87	0.686	0.067	73.4	18.2	18.2	1.09	1.22	1.46	162	48
	BH00R41	31	1	0.622	0.079	52.2	10.1	0.94	0.609	0.052	53.8	10.5	28.1	1.08	1.22	0.76	141	58
	BH00R41	33	1	0.569	0.074	41.3	6.9	0.82	0.526	0.051	40.5	13.1	38.7	1.07	1.51	0.62	83	35
	BH00R41	36	1	0.884	0.131	73.5	12.0	0.91	0.603	0.042	56.8	13.4	28.8	1.06	1.74	1.08	113	45
	BH00R41	38	1	1.05	0.10	92.9	10.5	0.88	0.640	0.034	37.5	6.8	24.1	1.05	1.73	0.85	178	93
La Vírgen	BH91B10	3	1	40.1	1.5	322	17	0.84	0.058	0.002	0.516	0.129	99.2	1.00	252[a]	4	238	126
	BH91B10	8	1	20.2	3.1	141	22	0.99	0.050	0.001	0.017	0.020	100.0	1.00	129[a]	1	656	423
	BH91B10	15	1	3.54	0.52	32.6	39.8	0.42	0.067	0.078	14.24	2.09	73.4	1.00	25.1[a]	3.5	269	133
	BH91B10	19	1	40.7	0.4	290	8	−0.28	0.052	0.002	0.590	0.217	99.1	1.00	255[a]	3	106	62
	BH91B10	10	1	0.050	0.008	5.07	1.06	0.81	0.734	0.090	93.61	42.73	12.1	3.25	0.127	0.081	195	98
	BH91B10	12	1	15.8	0.3	112	6	0.51	0.051	0.003	0.509	0.393	99.6	1.00	101[a]	1.7	74	42

Note: cc concordia error ellipse correlation coefficient.

f ^{230}Th disequilibrium correction factor calculated from $(Th/U)_{zircon}/(Th/U)_{melt}$ assuming $(Th/U)_{melt}=2.86$.

Slope of calibration curve Pb/U relative sensitivity vs. $UO^+/U^+=1.70$ ($n=10$; December 22 2003) and 2.31 ($n=7$; December 30 2003).

Reproducibility of AS-3 ^{206}Pb/^{238}U age = 2.7% 1 σ rel. (December 22 2003) and 4.2% (December 30 2003).

[a] ^{204}Pb corrected; all others ^{207}Pb corrected using common Pb compositions: $^{206}Pb/^{204}Pb=18.86$; $^{207}Pb/^{204}Pb=15.62$.

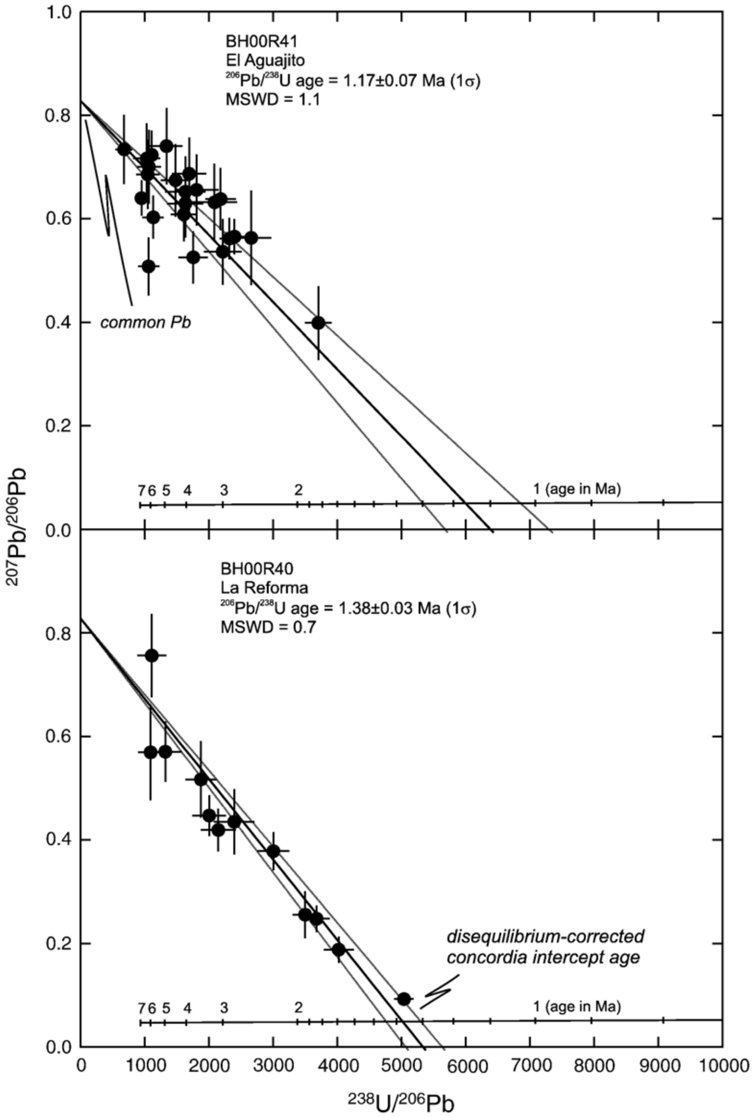

Fig. 6. $^{207}Pb/^{206}Pb$ vs. $^{238}U/^{206}Pb$ isochron diagram for Aguajito and La Reforma zircons. Concordia is corrected for initial disequilibrium (deficit in ^{230}Th) assuming a zircon–melt partitioning coefficient ratio $D_{Th}/D_U = 0.14$.

Vírgen deposit is difficult to evaluate without careful documentation of the field site. It could be a remnant root fragment from a plant growing on the deposit. Alternatively, it is conceivable that charcoal from wildfires could have been entrained by subsequent reworking of the La Vírgen deposit, e.g. by a landslide. Either of these scenarios could explain the younger date. In this context, it is also important to point out that He loss from La Vírgen zircons by post-depositional thermal events such as wildfires (Mitchell and Reiners, 2003) or emplacement of younger lava flows, can be ruled out because the sample was from a vertical section that is sufficiently insulated from the surface by several meters of overlying rocks, and younger lava flows are absent in the sample location.

In summary, we consider 36±3 ka as a reliable estimate for the age of the La Vírgen eruption that corroborates previous constraints from cosmogenic He dating. Historic accounts for a recent eruption of Tres Vírgenes may instead refer to landslides, steam release from hydrothermal activity (Capra et al., 1998), or potentially to an eruption of the latest summit andesite lava erupted from Las Tres Vírgenes. Furthermore, one of us (B. H.) received notification of a possible eruption of Volcán Tres Virgenes a few years ago that turned out to be a wild fire.

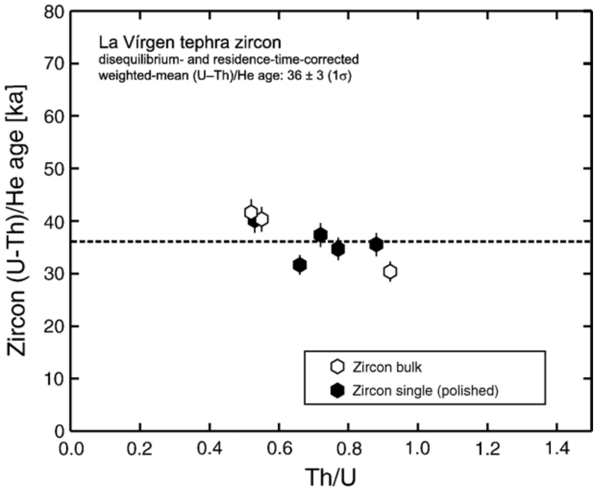

Fig. 7. Disequilibrium-corrected and residence-time-corrected (U–Th)/He ages for single and bulk zircon samples from La Vírgen tephra. Error bars (1σ) for individual (U–Th)/He symbols reflect measurement and α-ejection uncertainties only. The error for the weighted average (U–Th)/He age is scaled by the square-root of the MSWD (MSWD = 3.7; n = 8) to account for non-propagated uncertainties in residence time parameters, and assumes an uncertainty in the average U–Th zircon age of ~17%.

5.2. Pre-eruptive evolution and longevity of the La Vírgen magma system

In the first order, La Vírgen zircon ages fall into two groups: Late Pleistocene zircons with individual ages between ~300 and ~70 ka (Fig. 4), and xenocrystic zircons with ages significantly older than those from the Tres Vírgenes–Aguajito–La Reforma centers. The presence of xenocrystic zircons is clear evidence for crustal contamination in the La Vírgen magma system. By contrast, xenocrystic zircon is absent in Aguajito and La Reforma samples. This is surprising as La Reforma caldera contains Cretaceous granitic basement in its central resurgent block (Schmidt, 1975). While the lack of older zircon could be interpreted as a lack of crustal contamination of the Aguajito and La Reforma magmas, an alternative explanation could be that xenocrystic zircon became resorbed in a hot and zircon undersaturated melt at the early stages of magma generation. Further study using radiogenic (e.g., Sr, Nd, Pb) or stable (e.g., oxygen) isotopes might help to clarify this question.

U–Th and U–Pb zircon dating has revealed the presence of zircon populations whose crystallization significantly predates the eruption ages of their host rocks. As discussed above, the difference between (U–Th)/He and U–Th ages for La Vírgen indicates ~60,000–120,000 yr of crystal residence. The differences between U–Pb zircon and published K–Ar ages for Aguajito and La Reforma (Table 2) also suggest that zircon crystallization in these magmas significantly predates the eruptions, similar to evidence for pre-eruptive crystal residence in other silicic volcanic systems (e.g., Reid et al., 1997; Bindeman et al., 2001; Schmitt et al., 2003; Miller and Wooden, 2004; Bacon and Lowenstern, 2005). In those previous studies, the difference between zircon crystallization age and eruption age was based on the comparison between U–Th (U–Pb) ages of zircon and K–Ar (Ar–Ar) ages of high-K phases such as sanidine. Here, we demonstrated that U–Th and (U–Th)/He ages for the same materials yield estimates for pre-eruptive residence that agree well with those inferred from U–Th–Pb and K–Ar geochronology.

The presence of a multimodal zircon age distribution (Fig. 4) implies multiple episodes during which a magma batch cooled to its zircon saturation temperature of ~800 °C (using the calibration from Watson and Harrison, 1983, and La Vírgen pumice compositions from Sawlan, 1986 and Capra et al., 1998). If we assume that zircon crystallized during magma cooling at a shallow storage level, we can also conclude that no net temperature decrease occurred in this shallow magma storage zone over a period of at least ~120 ka. It is important to emphasize that over this time interval temperature fluctuations (heating and cooling cycles) are likely. In fact, rounding and partial resorption of zircon grains (including xenocrysts; Fig. 5) provide evidence for magma reheating to a temperature > 800 °C prior to the La Vírgen eruption. Crenulate margins of CL-visible domains also exist within grains (Fig. 5) and suggest multiple resorption and overgrowth events over the ~10–100 ka lifetime of the magma system. This is consistent with petrographic evidence that evolved silicic melt mixed with less evolved recharge magma prior to the eruption and thus became thermally rejuvenated (Capra et al., 1998).

It is difficult to decide if crystals continuously resided in a magma or partially crystallized mush or if they became recycled by remelting of solidified earlier intrusions. The age gap between the younger peak in the zircon U–Th age distribution and the eruption age (Fig. 4) may indicate that zircon crystallization ceased due to freezing of a silicic intrusion but continuous magma residence cannot be completely ruled out in the case that our sampling overlooked the youngest zircon growth episodes. The absence of zircon ages equivalent to those present in Aguajito and La Reforma ignimbrites, however, clearly indicates that the La Vírgen eruption tapped a magma reservoir that was separate from and significantly younger than those of Aguajito and La Reforma.

U–Th zircon ages allow us to refine existing models for the Las Tres Vírgenes magma system. Mantle melting and basaltic underplating related to crustal extension, decompression, and nascent oceanic spreading within the Gulf of California rift zone (Batiza, 1979; Capra et al., 1998) represents a regionally long-lived heat source that sustained crustal melting and assimilation intermittently over periods of more than ~1 Million years. Emplacement of multiple, individually short-lived evolved magma batches at shallow crustal level occurred over time scales of 10,000 to 100,000 years that eventually culminated in a thermal rejuvenation event by recharge of basaltic magma and the amassment of several km^3 of rhyodacitic magma (Capra et al., 1998). In the light of the relatively young eruption age and geochronologic evidence for the existence of a long lived thermal anomaly at Volcán Las Tres Vírgenes, future eruptions should be anticipated.

6. Conclusions

(1) Holocene (Capra et al., 1998) eruption of Las Tres Vírgenes volcano is inconsistent with disequilibrium-corrected (U–Th)/He zircon results for La Vírgen tephra that indicate an eruption age of 36±3 ka; younger andesite summit lavas could possibly account for the historic report (Ives, 1962);
(2) (U–Th)/He zircon ages for the voluminous La Vírgen tephra are consistent with the cosmogenic He exposure age (26±4 ka; Hausback and Abrams, 1996) of an overlying basalt lava, suggesting a near continuous eruption sequence;
(3) Zircon U–Th disequilibrium model ages of La Vírgen tephra predate the eruption by ~60,000–120,000 yr. Partially resorbed zircon, an apparent gap between zircon crystallization and eruption ages, and multimodal U–Th zircon ages imply episodic zircon crystallization over several 10,000 years. Despite differences in their tectonic settings, the longevity of the heat source that sustained episodic intrusions and reheating at Las Tres Vírgenes is comparable to what is observed for composite volcanoes in active arcs (e.g., Mt. Mazama; Bacon and Lowenstern, 2005);
(4) Earlier silicic ignimbrites that erupted from the adjacent Aguajito and La Reforma calderas yielded Early Pleistocene ages. Equivalent ages are absent among Las Tres Vírgenes zircons. By contrast, xenocrystic zircon is common in La Vírgen tephra. This implies a separate magma chamber for the La Vírgen magma system and a significant role of basement assimilation;
(5) The time-interval for pre-eruptive zircon growth and residence considerably exceeds the period of recent dormancy. Thus, future eruptive activity of Las Tres Vírgenes volcano appears consistent with its geologic history. Las Tres Virgenes is a potentially active volcano.

Acknowledgments

We thank Charles Bacon and an anonymous referee for their constructive reviews, and Bruce Marsh for the editorial handling of the manuscript. Lisa Stockli (University of Kansas) is thanked for her analytical support. Haibo Zou (UCLA) provided valuable assistance in the clean room facility. The ion microprobe facility at UCLA is partly supported by a grant from the Instrumentation and Facilities Program, Division of Earth Sciences, National Science Foundation.

Appendix A. U–Th ion microprobe analysis: Background corrections, standard reproducibility, and comparison to LA-ICP-MS techniques

U–Th ion microprobe dating of zircon utilizes the high sensitivity of secondary ionization mass spectrometry that is presently unrivaled by any other technique. Typically, 0.02 μg of zircon are consumed during a ~30 min analysis (at a sputter rate for an O^- primary beam of ~0.05 μm^3/nA/s), whereas LA-ICP-MS measurements require ~10 μg (Stirling et al., 2000). ThO^+ is chosen for analysis, because it is ~10 times more abundant than Th^+ during sputtering of zircon with O^-. The useful yield for ThO^+ is ~1.3% in ion microprobe techniques, compared to ~0.3% for LA-ICP-MS ($^{238}U^+$; Stirling et al., 2000).

The Th–U sensitivity is calibrated by measuring $^{208}Pb/^{206}Pb$ on concordant reference zircons (AS-3 and 91500; Paces and Miller, 1993; Wiedenbeck et al., 1995). In contrast to U–Pb dating of zircon where analytical precision is in many cases limited by the ability to monitor the U–Pb instrumental sensitivity (usually by calibrating the U–Pb relative sensitivity against UO^+/U^+), the observed variability in Th–U sensitivity is smaller, typically <1.4%. Instead, precision and accuracy are practically limited by counting statistics on $^{230}ThO^+$ (~0.2–5 cps) and the ability to perform an adequate correction for background. Sources for background on $^{230}ThO^+$ include electron multiplier (EM) dark noise, scattered ions, and unresolved interferences ($^{232}Th_2CO^{2+}$). Fig. 8 shows that $^{232}Th_2CO^{2+}$ is commonly insignificant on pure, Au-coated zircon, but can overwhelm the $^{230}ThO^+$ signal if

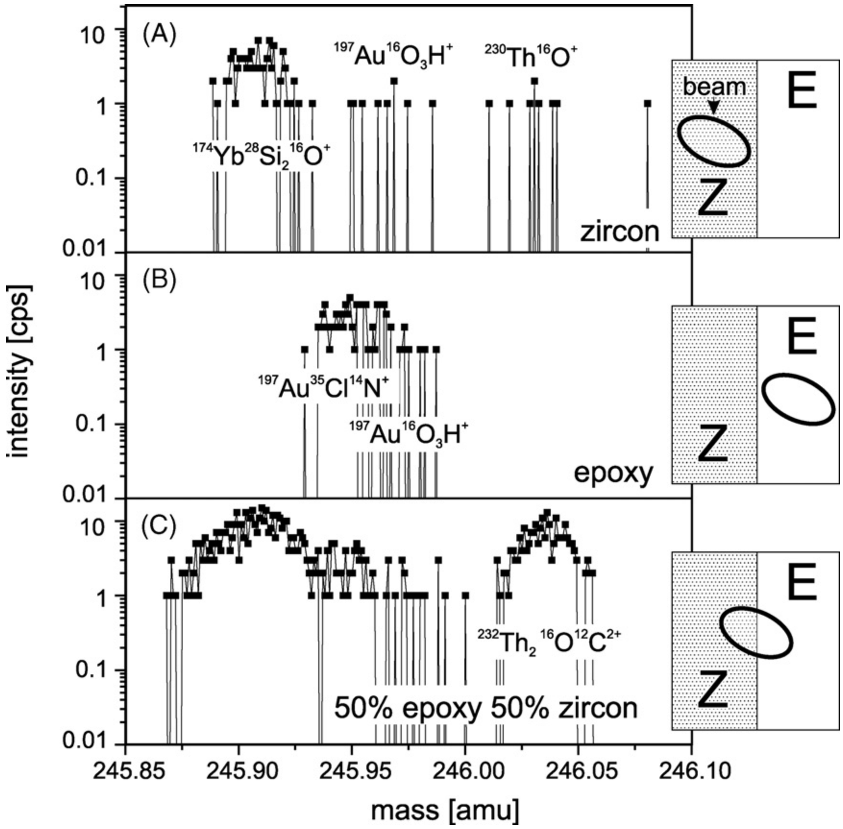

Fig. 8. High-mass resolution scans ($M/\Delta M = \sim 5000$) of (A) low-U zircon (G42728A with 24 ppm U; Wiedenbeck et al., 1995), (B) epoxy, and (C) area with primary beam overlapping epoxy and zircon in approximately equal proportions. Primary beam (O^-) intensity ~40 nA.

carbon is been made available within the sputtered region. Thus, carbon coating or beam overlap with the epoxy mounting medium has to be rigorously avoided. In order to monitor $^{232}Th_2CO^{2+}$, an additional mass station at 244.038 amu is included in the analysis protocol where the presence of $^{232}ThC^+$ can be detected. A second background mass station (246.300) is included to record EM dark noise and scattered ions adjacent to the $^{230}ThO^+$ peak (246.028 amu). Typical background count rates recorded on standard zircons are: 0.03 cps (246.300) and 0.07 cps (244.038). (^{230}Th)/(^{238}U) results for AS-3 and 91 500 analyzed throughout the analytical period are summarized in Table 4. From this, it becomes obvious that using either the 246.300 or the averaged background from 246.300 and 244.038 yields average (^{230}Th)/(^{238}U) ratios that are accurate within ~1.7% (1σ mean). No background and 244.038 only corrections, by contrast, tend to overestimate and underestimate (^{230}Th)/(^{238}U) by ~3%, respectively.

For a typical ~30 min analysis, the in-run precision of (^{230}Th)/(^{238}U) for AS-3 standards averaged ~6% (1σ rel.; average U concentration ~700 ppm), and ~14% for low-U 91 500 zircon (81.2 ppm U). Overall, the reproducibility on both standards is ~6% (1 standard deviation; MSWD = 0.8), compared to ~2% for LA-ICP-MS (Stirling et al., 2000). It should be noted, however, that the material required for LA-ICP-MS is ~500 times that of an ion microprobe analysis, rendering individual crystal analysis as performed in this study impossible for current LA-ICP-MS techniques.

Table 4
Summary of (^{230}Th)/(^{238}U) results for standard zircons 91,500 and AS-3 calculated using different background correction schemes

Correction on mass 246.029	(^{230}U)/(^{232}Th)	±	MSWD
No background	1.036	0.016	1.7
246.300 only	1.001	0.017	0.7
244.038 only	0.969	0.017	1.1
Average of 246.300 and 244.038	0.985	0.017	0.8

Data acquired between Dec 2003 and Feb 2005. Total number of analyses: $n = 14$ (AS-3: $n = 8$; 91500: $n = 6$).
ThO^+/UO^+ relative sensitivity factors between 0.88 and 0.95.
Decay constants used: λ_{230}: 9.1577×10^{-6} a^{-1}; λ_{238}: 1.55125×10^{-10} a^{-1}.

References

Bacon, C.R., Lowenstern, J.B., 2005. Late Pleistocene granodiorite source for recycled zircon and phenocrysts in rhyodacite lava at Crater Lake, Oregon. Earth and Planetary Science Letters 233, 277–293.

Batiza, R., 1979. Trace element and strontium isotope characteristics of volcanic rocks from Isla Tortuga: a young seamount in the Gulf of California. Earth and Planetary Science Letters 43, 269–278.

Bindeman, I.N., Valley, J.W., Wooden, J.L., Persing, H.M., 2001. Post-caldera volcanism; in situ measurement of U–Pb age and oxygen isotope ratio in Pleistocene zircons from Yellowstone Caldera. Earth and Planetary Science Letters 189 (3–4), 197–206.

Bird, M.I., Turney, C.S.M., Fifield, L.K., Jones, R., Ayliffe, L.K., Palmer, A., Cresswell, R., Robertson, S., 2002. Radiocarbon analysis of the early archaeological site of Nauwalabila I, Arnhem Land, Australia: implications for sample suitability and stratigraphic integrity. Quaternary Science Reviews 21 (8–9), 1061–1075.

Capra, L., Macias, J.L., Espindola, J.M., Siebe, C., 1998. Holocene plinian eruption of La Virgen Volcano, Baja California, Mexico. Journal of Volcanology and Geothermal Research 80 (3–4), 239–266.

Demant, A., 1981. Plio–Quaternary volcanism of the Santa Rosalia area, Baja California, Mexico. In: Ortlieb, L., Roldan-Quintana, J. (Eds.), Geology of Northwestern Mexico and Southern Arizona; Field Guides and Papers. U.N.A.M, Inst. Geol., Estacion Regional del Noroeste, Mexico City, Mexico D.F., pp. 295–307.

Demant, A., 1984. The Reforma Caldera, Santa Rosalia area, Baja California. A Volcanological, petrological, and mineralogical study. In: Malpica-Cruz, V., Celis-Gutierrez, S., Guerrero-Garcia, J., Ortlieb, L. (Eds.), Neotectonics and sea level variations in the Gulf or California area. Univ. National Auton, Mexico, Inst. Geologia, Mexico D.F., pp. 75–96.

Fabriol, H., Delgado-Argote, L.A., Danobeitia, J.J., Cordoba, D., Gonzalez, A., Garcia-Abdeslem, J., Bartolome, R., Martin-Atienza, B., Frias-Camacho, V., 1999. Backscattering and geophysical features of volcanic ridges offshore Santa Rosalia, Baja California Sur, Gulf of California, Mexico. Journal of Volcanology and Geothermal Research 93 (1–2), 75–92.

Farley, K.A., Wolf, R.A., Silver, L.T., 1996. The effects of long alpha-stopping distances on (U–Th)/He ages. Geochimica et Cosmochimica Acta 60 (21), 4223–4229.

Farley, K.A., Kohn, B.P., Pillans, B., 2002. The effects of secular disequilibrium on (U–Th)/He systematics and dating of Quaternary volcanic zircon and apatite. Earth and Planetary Science Letters 201 (1), 117–125.

Garduño-Monroy, V.H., Vargas-Ledezma, H., Campos-Enriquez, J.O., 1993. Preliminary geologic studies of Sierra El Aguajito (Baja California, Mexico): a resurgent-type caldera. Journal of Volcanology and Geothermal Research 59 (1–2), 47–58.

Hausback, B.P., 1984. Cenozoic volcanic and tectonic evolution of Baja California Sur, Mexico. In: Frizzell Jr., V.A. (Ed.), Geology of the Baja California Peninsula. Society of Economic Paleontologists and Mineralogists, Pacific Section, Los Angeles, CA, pp. 219–236.

Hausback, B.P., Abrams, M.J., 1996. Plinian eruption of La Virgen Tephra, Volcán Las Tres Virgenes, Baja California Sur, Mexico. Eos, Transactions, American Geophysical Union 77 (46, Suppl.), 813–814.

Hook, S.J., Dmochowski, J.A., Howard, K.A., Rowan, L.C., Karlstrom, K.E., Stock, J.M., 2005. Mapping variations in weight percent silica measured from multispectral thermal infrared imagery — Examples from the Hiller Mountains, Nevada, USA and Tres Virgenes–La Reforma, Baja California Sur, Mexico. Remote Sensing of Environment 95, 273–289.

Ives, R.L., 1962. Dating of the 1746 eruption of Tres Virgenes Volcano, Baja California del Sur, Mexico. Geological Society of America Bulletin 73 (5), 647–648.

Layne, G.D., Sims, K.W., 2000. Secondary ion mass spectrometry for the measurement of $^{232}Th/^{230}Th$ in volcanic rocks. International Journal of Mass Spectrometry 203, 187–198.

Mahon, K., 1996. The New 'York' regression: application of an improved statistical method to geochemistry. International Geological Review 38, 293–303.

Martín-Barajas, A., Stock, J.M., Layer, P., Hausback, B., Renne, P., López-Martínez, M., 1995. Arc-rift transition volcanism in the Puertecitos volcanic province, northeastern Baja California, Mexico. Geological Society of America Bulletin 107, 407–424.

Medina, F., Suarez, F., Espindola, J.M., 1989. Historic and holocene volcanic centers in NW Mexico: a supplement to the IAVCEI catalogue. Bulletin of Volcanology 51 (Suppl. 1), 91–93.

Miller, J.S., Wooden, J.L., 2004. Residence, resorption and recycling of zircons in Devils Kitchen Rhyolite, Coso volcanic field, California. Journal of Petrology 45 (11), 2155–2170.

Mitchell, S.G., Reiners, P.W., 2003. Influence of wildfires on apatite and zircon (U–Th)/He ages. Geology 31 (12), 1025–1028.

Paces, J.B., Miller, J.D., 1993. Precise U–Pb ages of Duluth Complex and related mafic intrusions, northeastern Minnesota; geochronological insights to physical, petrogenetic, paleomagnetic, and tectonomagnetic processes associated with the 1.1 Ga Midcontinent Rift System. Journal of Geophysical Research 98, 13997–14013.

Portugal, E., Birkle, P., Barragan, R.R.M., Arellano, G.V.M., Tello, E., Tello, M., 2000. Hydrochemical-isotopic and hydrogeological conceptual model of the Las Tres Virgenes geothermal field, Baja California Sur, Mexico. Journal of Volcanology and Geothermal Research 101 (3–4), 223–244.

Quijano-León, J.L., Gutiérrez-Negrín, L.C.A., 2003. An unfinished journey: 30 years of geothermal-electric generation in mexico. Geothermal Resources Council Bulletin 32, 198–203.

Reid, M.R., Coath, C.D., Harrison, T.M., McKeegan, K.D., 1997. Prolonged residence times for the youngest rhyolites associated with Long Valley Caldera; 230Th–238U ion microprobe dating of young zircons. Earth Planetary Science Letters 150, 27–39.

Russell, I.C., 1897. Volcanoes of North America; A Reading Lesson for Students of Geography and Geology. Macmillan, New York. 346 pp.

Sambridge, M.S., Compston, W., 1994. Mixture modeling of multi-component data sets with application to ion probe zircon ages. Earth and Planetary Science Letters 128, 373–390.

Saunders, A.D., Rogers, G., Marriner, G.F., Terrell, D.J., Verma, S.P., 1987. Geochemistry of Cenozoic volcanic rocks, Baja California, Mexico; implications for the petrogenesis of post-subduction magmas. Journal of Volcanology and Geothermal Research 32 (1–3), 223–245.

Sawlan, M.G., 1986. Petrogenesis of Late Cenozoic Volcanic Rocks from Baja California Sur, Mexico. Doctoral Thesis, University of California, Santa Cruz.

Sawlan, M.G., 1991. Magmatic evolution of the Gulf of California rift. AAPG Memoir 47, 301–369.

Schmidt, E.G., 1975. Plate tectonics, volcanic petrology, and ore formation in the Santa Rosalia area, Baja California, Mexico. Masters Thesis, University of Arizona, Tucson.

Schmitt, A.K., Grove, M., Harrison, T.M., Lovera, O., Hulen, J., Walters, M., 2003. The Geysers–Cobb Mountain Magma System, California (Part 1): U–Pb zircon ages of volcanic rocks, conditions of zircon crystallization and magma residence times. Geochimica et Cosmochimica Acta 67, 3423–3442.

Siebert, L., Simkin, T., 2002–2005. Volcanoes of the World: an Illustrated Catalog of Holocene Volcanoes and their Eruptions. Smithsonian Institution, Global Volcanism Program Digital Information Series, GVP-3, (http://www.volcano.si.edu/world/).

Stirling, C.H., Lee, D.-C., Christensen, J.N., Halliday, A.N., 2000. High-precision in situ 238U–234U–230Th isotopic analysis using laser ablation multiple-collector ICPMS. Geochimica et Cosmochimica Acta 64 (21), 3737–3750.

Umhoefer, P.J., Dorsey, R.J., Willsey, S., Mayer, L., Renne, P.R., 2001. Stratigraphy and geochronology of the Comondu Group near Loreto, Baja California Sur, Mexico. Sedimentary Geology 144, 125–147.

Watson, E.B., Harrison, T.M., 1983. Zircon saturation revisited; temperature and composition effects in a variety of crustal magma types. Earth Planetary Science Letters 64, 295–304.

Wiedenbeck, M., Allé, P., Corfu, F., Griffin, W.L., Meier, M., Oberli, F., Von Quadt, A., Roddick, J.C., Spiegel, W., 1995. Three natural zircon standards for U–Th–Pb, Lu–Hf, trace element and REE analyses. Geostandards Newsletter 91, 1–23.